czewski, Phys. Letters 31A, 56 (1970); Acta Phys. Polon. A40, 505 (1971).

[5]Y. L. Wang, D. Yang, and M. R. H. Khajehpour, J. Appl. Phys. 42, 1418 (1971).

[6]J. W. Stout and W. B. Hadley, J. Chem. Phys. 40, 55 (1964).

[7]A. Herweijer and S. A. Friedberg, Phys. Rev. B 4, 4009 (1971).

[8]M. Blume, V. J. Emery, and R. B. Griffiths, Phys. Rev. A 4, 1071 (1971).

[9]B. D. Rainford and J. G. Houmann, Phys. Rev. Letters 26, 1254 (1971).

[10]Y. L. Wang (unpublished).

[11]L. D. Landau and E. M. Lifschitz, Statistical Physics, 2nd ed. (Addison Wesley, Readings, Mass., 1969), p. 424.

[12]G. T. Trammell, J. Appl. Phys. 31, 362S (1960); B. Bleaney, Proc. Roy. Soc. (London) 276A, 19 (1963); Y. L. Wang and B. R. Cooper, Phys. Rev. 172, 539 (1968); 185, 696 (1969).

Experimental and Calculated Photoelectron Energy-Distribution Curves of Ni above and below the Curie Temperature*

D. T. Pierce[†] and W. E. Spicer

Stanford University, Stanford, California 94305

(Received 17 January 1972)

Theoretical photoelectron energy-distribution curves (EDC) of Ni were calculated using an interpolated band structure with an exchange splitting of the ferromagnetic bands of 0.37 eV at E_F. From paramagnetic to ferromagnetic Ni, the leading peak of the EDC originating from d bands near E_F is predicted to shift 0.25 eV over the range $7.7 \leq \hbar\omega \leq 10.7$ eV (assuming direct transitions) and 0.18 eV (assuming nondirect transitions). High-resolution photoelectron spectra obtained from ferromagnetic Ni (295 °K, $0.47T_C$) and paramagnetic Ni (678 °K, $1.07T_C$) gave no evidence of a significant change in the amplitude nor of a change in the position of the d-electron peak near the high-energy cutoff of the EDC within the experimental uncertainty of ± 0.05 eV. High-temperature EDC were obtained from continuously heated Ni single crystals and electron-gun-evaporated films, using a screened-emitter energy analyzer. These results are compared to related experiments, and it is concluded that the band model of magnetism does not adequately explain Ni photoemission and optical experiments.

I. INTRODUCTION

This paper is a complete report on our photoemission measurements from Ni above and below the Curie temperature. These measurements were briefly described previously.[1] The d-band peak in the photoelectron energy-distribution curves (EDC) did not exhibit the temperature dependence predicted by our calculations based on the band model of ferromagnetism. The band theory of itinerant-electron ferromagnetism, which originated with Slater[2] and Stoner[3] and was further developed by Wohlfarth,[4] assumes an approximately rigid energy splitting of the spin subbands that is temperature dependent below and zero above T_C.

The difference in energy between states of opposite spin at the same wave vector $\vec{k}$ in corresponding spin subbands is frequently referred to as "exchange splitting," although the relative importance of contributions from different types of exchange and correlation effects is uncertain. Wohlfarth[5] has tabulated the exchange-splitting estimates derived from various experimental and theoretical work, including measurements of specific heat, susceptibility, saturation magnetization, op-

tical properties, and calculations of band structures. From examination of values ranging from 0.21 to 1.7 eV, he concluded that the best estimate is 0.35 ± 0.05 eV. Phillips[6] has more recently extended Wohlfarth's table, and placing more emphasis on the band calculations and Fermi-surface models as opposed to macroscopic quantities, he arrived at a larger exchange-splitting estimate of 0.5 ± 0.1 eV. The Hartree-Fock approximation, which is the basis of the band theory of ferromagnetism, must be inadequate to some degree, because the wave functions do not account for the correlation between electrons of antiparallel spin that results from the Coulomb repulsion between them. Consequently, there can be, with reasonable probability, an excess of charge on one atom and a deficiency on another. The extent of such polarity fluctuations depends on the relative magnitudes of the polarity energy (which is the Coulomb repulsion between two d electrons with antiparallel spin on the same atom) and of the hopping energy (the energy of an electron hopping from one site to the next which is approximately as large as the band-width). Herring[7] discussed in some detail the rivalling points of view on the strength of correlation ef-

fects; there appears to be agreement on the fact that the exchange splitting between up-spin and down-spin states is predominantly the result of the intra-atomic Coulomb energy.

The band model explains many of the magnetic properties of Ni, notably the nonintegral saturation moment. The band model of magnetism, however, has not been able to explain such recent findings as our results and the complementary experiments on cesiated Ni of Rowe and Tracy[8] nor the spin-polarized photoelectron measurements.[9] These experiments, the apparent conflict noted previously[1] between our results and those from optical absorption,[10] and the neutron-scattering experiments[11] are described in Sec. IV.

In Sec. II we discuss our calculation of the predicted peak shifts in the EDC. From the direct-transition model of the optical-excitation process, one expects a 0.25-eV shift, and from the nondirect-transition model, a 0.18-eV shift. In Sec. III we present our method of obtaining the first high-resolution measurements of Ni above the Curie temperature T_C. The experimental results reveals that no peak shift is observed within our experimental uncertainty of ±0.05 eV.

II. THEORY

To obtain an understanding of the magnitude of the difference that might be expected in EDC measured at room temperature and above the Curie temperature, we have calculated EDC on the basis of the Slater-Stoner-Wohlfarth band model. These calculations were made using two models for the optical-excitation process in Ni: the direct-transition model and the nondirect-transition model.[12,13] The interpolation scheme of Hodges, Ehrenreich, and Lang[14] provided the nickel band structure that must be known throughout the entire Brillouin zone so as to calculate the EDC. The parameters of the model Hamiltonian were determined by Ehrenreich and Hodges[15] (set b) by fitting to the first-principles augmented-plane-wave (APW) paramagnetic calculation of Hanus[16] at symmetry points. A slight adjustment of three of the 14 parameters was made to obtain better agreement with experimental data from (i) neutron-diffraction determination of the magnetic form factor, (ii) de Haas-van Alphen measurements, (iii) magneto-optical measurements, (iv) measurements of thermally modulated reflectivity, and (v) the ferromagnetic Kerr effect.[14] The basic set used consisted of four orthogonalized plane waves representing the conduction bands and five linear combinations of atomic orbitals representing the d bands in a tight-binding approximation. This interpolation scheme affords significant computational advantages, because only a (9×9)-model Hamiltonian matrix must be diagonalized at each point in k space in the paramagnetic calcu-

lation. Because the spin-orbit coupling is small, the electron spin is not changed to first order in the optical transition, and the 18×18 ferromagnetic Hamiltonian matrix reduces to two 9×9 matrices (one for each spin).

Hodges et al.[14] calculated a k-dependent splitting of the ferromagnetic bands, which amounts to 0.37 eV for states near E_F and 0.29 eV averaged throughout the zone. The difference occurs because the splitting of the bands for states of E_g symmetry is 0.1 eV, and the splitting of the bands for states of T_{2g} symmetry (those that are predominant at the Fermi level) is 0.42 eV. In the band model, the difference in energy between electrons of opposite spins is related to the magnetization and assumed to go to zero at the Curie temperature. The EDC calculated by using the paramagnetic band structure are to be compared to our EDC measured above T_C, and the EDC calculated for the ferromagnetic band structure at zero temperature (100% magnetization) are to be compared to EDC measured at room temperature (95% magnetization).

Given the nickel band structure throughout the Brillouin zone, we followed the procedure of Smith[17,18] to calculate the EDC in the direct-transition model; wave vector $\vec{k}$ is conserved in this model, which corresponds to "vertical" transitions between initial and final states at the same point in k space in the reduced zone scheme. Each absorbed photon is assumed to excite an electron from an initial state of energy $E_i(\vec{k})$ in band i to a final state of energy $E_f(\vec{k})$ in band f. The energy distribution of photoexcited electrons is

$$D(E_i, \omega) = C \sum_{i,f} \int d^3k \, |M|^2 \delta(E_f(\vec{k}) - E_i(\vec{k}) - \hbar\omega)$$

$$\times \delta(E - E_i(\vec{k})) F_i (1 - F_f) , \quad (1)$$

where $\hbar\omega$ is the photon energy, F is the Fermi function, and C is a constant. The integral in k space is over the Brillouin zone.

In our calculation, as in past direct-transition calculations of EDC,[17-19] we made the approximation that the matrix element M is a constant. Some cases in which this approximation has important consequences are discussed below. Only recently, matrix elements have been included in such a calculation for the first time in the work of Williams et al. on copper.[20]

The joint density of states (JDOS) is defined by

$$J(\omega) = \sum_{i,f} \int \frac{2}{(2\pi)^3} \delta(E_f(\vec{k}) - E_i(\vec{k}) - \hbar\omega) d^3k .$$

$$(2)$$

In this constant-matrix-element approximation, $D(E, \omega)$ is the energy distribution of the joint density of state (EDJDOS). For a direct-transition model, Smith[16] and Eastman[21] have emphasized that

the experimental EDC sense the EDJDOS, rather than the density of states (DOS) given by

$$\eta(E) = \frac{2}{(2\pi)^3} \sum_i \int d^3k \, \delta(E - E_i(\vec{k})) .$$ (3)

Another significant quantity that we calculated and compared to experiment is the imaginary part of the dielectric constant $\epsilon_2(\omega)$. In the constant-matrix-element approximation, $\epsilon_2(\omega)$ is related simply to the JDOS by $\epsilon_2(\omega) \propto J(\omega)/\omega^2$.

To compute the integral of Eq. (1) over the Brillouin zone, the primitive $\frac{1}{48}$ of the zone was divided into cubes of size such that there were 17 cubes in-going from the one centered at Γ to the one centered at X inclusively. The sample point is taken to be representative of the entire cube. For sample points that fall at points of special symmetry (such as a zone edge or plane), only part of the surrounding cube lies within the $\frac{1}{48}$ of the zone. The contributions from the cubes are weighted accordingly; for example, the cube at Γ is weighted $\frac{1}{48}$ as much as a general point. A linear interpolation[18] of the band structure was used in each of these cubes. The 9×9 Hamiltonian matrix was diagonalized at the cube center $\vec{k}_0$ and at three nearby points Δk away in the $k_x, k_y,$ and k_z directions. Each cube was then divided into 343 (i.e., 7^3) subcubes. The energy of a band j at the center of each subcube was found from

$$E_j(\vec{k}) = E_j(\vec{k}_0) + (\vec{k} - \vec{k}_0) \cdot \vec{\nabla}_k E_j(\vec{k}_0) .$$ (4)

The size of Δk used in calculating the derivative is limited on the small side by the accuracy to which the energy eigenvalues are calculated and on the large side by the aim to minimize errors in computing derivatives near band crossings. A value for Δk corresponding to $\frac{1}{20}$ of a cube edge was used in these calculations.

At this point in the calculation, there are nine energy values at each of 173 215 (343×505) points in the $\frac{1}{48}$ irreducible zone. The quantities of interest are calculated in histogram form. The energy values were put in histogram boxes of set width by going from real to integer base on the computer. The $D(E, \omega)$ is found by cataloging transitions according to the initial state energy and the photon energy separating the initial and final state. A grid of 0.05 eV was used for both the initial state energy and the photon energy. The part of the EDC corresponding to states near the Fermi level was modified by the Fermi distribution at the approach temperature (300 or 678 °K).

To obtain the energy distribution of *photoemitted* electrons from the distribution of *photoexcited* electrons in Eq. (1), we must consider how the distribution is modified by electron transport to the surface and escape over the surface barrier. A semiclassical threshold function $T(E, \omega, \vec{k})$ can

be calculated by taking account of the depth at which the electron is excited, the probability of a collision during travel to the surface, and the minimum momentum normal to the surface required to overcome the surface barrier. Rigorously, the threshold function should be included in the k-space integral of Eq. (1), but in the random $\vec{k}$ approximation, it is independent of $\vec{k}$ and can be calculated separately.[12,22] In nickel, the collision probability is determined by the electron-electron–scattering length which was set equal to 10 Å for electrons with energies of 8.0 eV above E_F and assumed to vary as $E^{1/2}/(E - E_F)^2$. This yields scattering lengths in good agreement with the 5-to-15-Å variation in Ni above 7 eV, as reported by Eastman.[23] The general shape of the threshold function, which is of importance in comparing our calculations to our experiments, is not very sensitive to the exact magnitude or energy dependence of the scattering length.

The distribution of photoemitted electrons obtained by applying the threshold function to $D(E_i, \omega)$ is modified further by the measurement process because of the spectral breadth of the exciting radiation and the finite resolution of the electron-energy analyzer.[24] To make a better comparison with experiment, the calculated energy-distribution histograms were convolved with a broadening function.[25]

A representative selection of the resulting calculated EDC is shown in Fig. 1, in which the ferromagnetic curves (solid) lie below the paramagnetic curves (dashed) at the same photon energies. The zero of energy is taken at the Fermi level. These curves exhibit the following striking features: (i) There is a large amount of structure. (ii) The strength of some pieces of structure changes dramatically with photon energy. (iii) The leading peak near the Fermi level is present and strong in all of the curves. (iv) Significant differences occur between pieces of structure in the ferromagnetic and paramagnetic curves. (v) Large pieces of structure appear at positions without corresponding structure in the density of states (see Fig. 7). A detailed comparison with experiment will be given in Sec. III; however, we note that the experimental data reveal a strong leading peak at 0.3 to 0.4 eV below the Fermi level and a broad lower bump at approximately 2.0 eV below the Fermi level. Neither the large amount of structure nor the change in strength of structure with photon energy is seen in the experimental curves. As a result, in using the calculated curves to predict what changes might be expected in going above the Curie temperature, we will neglect differences in low-energy structure and concentrate on the leading peak which is strong in both the calculated curves and in experiment.
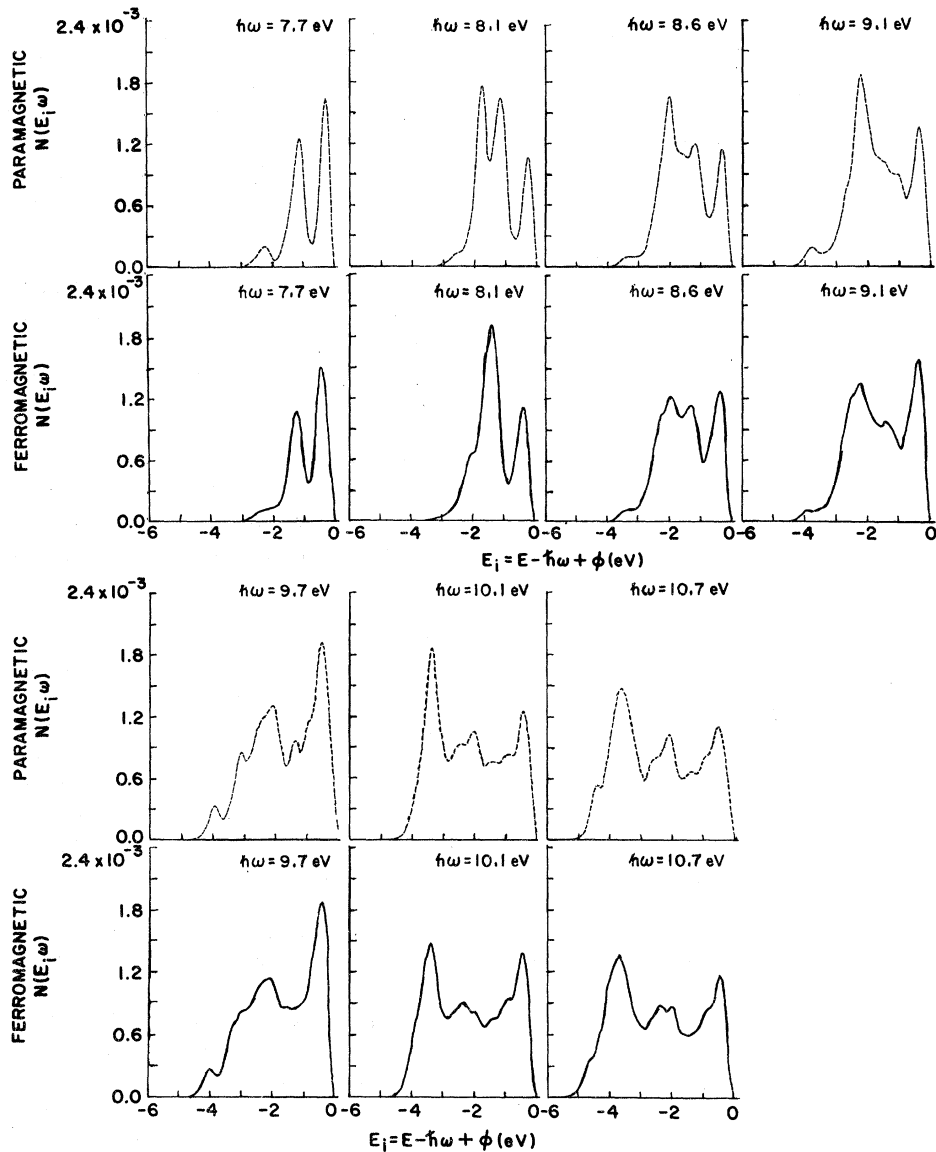
FIG. 1. Representative calculated EDC for Ni, assuming direct transitions and the Ni band structure of Hodges *et al.*, which has an exchange splitting of 0.37 eV at E_F. The upper (dashed) curves are for paramagnetic Ni and the lower (solid) curves are for ferromagnetic Ni at corresponding photon energies. The leading peak near E_F (zero of energy scale) is present in all the curves.

The changes in experimental EDC above T_C which would be expected on the basis of these calculations, are revealed in the close comparison of the calculated curves in Fig. 2. The insert in the figure is a 3× magnification of the leading peak. The leading peak of the paramagnetic nickel nearly lines up in energy with the peak of ferromagnetic nickel at a photon energy of $\hbar\omega = 9.1$ eV, but the leading peak in the calculated paramagnetic curve is shifted 0.16 eV higher in energy for $\hbar\omega = 7.7$ and 0.09 eV lower in energy for $\hbar\omega = 10.7$ eV. This rather surprising relative shift of the peak positions demonstrates the importance in the direct-transition

model of the unfilled states to which the electrons are excited.

The experimental curves in Sec. III show little of the calculated structure displayed in Fig. 1. The width of the calculated structure is such that, if present, it would be easily resolved in the experiment as is the leading peak. The discrepancy may be attributed in part to our assumption of constant matrix elements; for example, the large peak in the calculated EDC somewhat more than 2 eV below E_F in the range $\hbar\omega = 8.6$–9.9 eV could be caused by transitions near the L_{31}-to-L_{12} transition. This transition, however, is from a d-like to an s-like
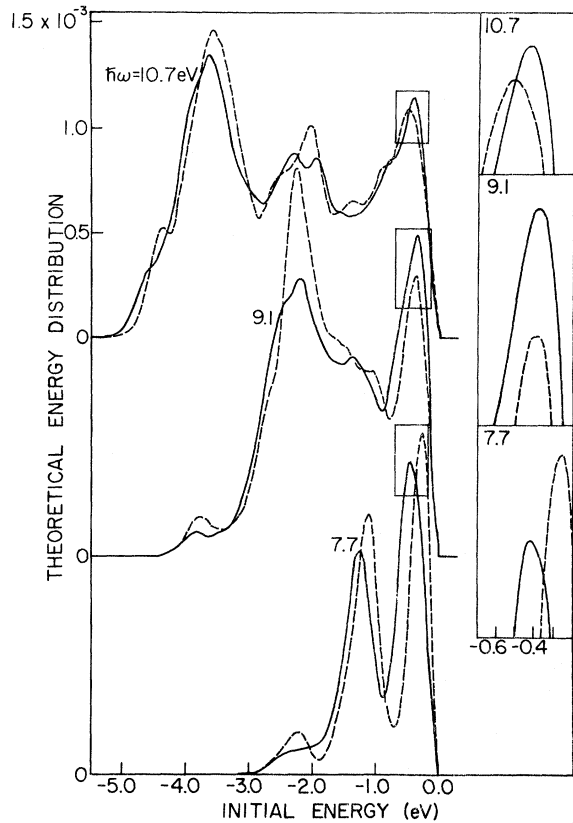
FIG. 2. Close comparison of three curves in Fig. 1 to determine the shift of the d-band peak near E_F in going from ferromagnetic (solid curves) to paramagnetic (dashed curves) Ni. The inserts (3× magnifications of the leading peaks) indicate that the paramagnetic peak shifts 0.25 eV relative to the ferromagnetic peak between $\hbar\omega = 7.7$ and 10.7 eV.

state and therefore is "forbidden." The matrix element calculated by Mueller and Phillips[26] for such a transition in copper is very small, which could be the reason for the absence of such a strong peak in the experimental curve. Because EDC are due to transitions over a region of k-space, it would be presumptuous to identify transitions from a band diagram along single lines in k space, and, of course, one must be cautious in this regard.

The difference to be expected in EDC from ferromagnetic and paramagnetic nickel also can be estimated in terms of the nondirect-transition model of the optical-transition process. The essence of the nondirect-transition model is that the conservation of wave vector $\vec{k}$, in a one-electron sense, is not a significant selection rule. The optical-transition probability from an initial state energy E_i with photon energy $\hbar\omega$ is

$$P(E_i, \omega) = \eta(E_i)\, \eta(E_i + \hbar\omega)/\omega\sigma(\omega) , \qquad (5)$$

where the rate of energy absorption $\omega\sigma(\omega)$ is a normalizing factor. The $\eta(E)$ is defined as the

"optical density of states" which may be different from the true ground-state densities $n(E)$, because of the effects of the matrix elements that have been absorbed into the optical DOS or because of the many-body effects outside of this one-electron picture.[13] As in the direct-transition case, to obtain the energy distribution of photoemitted electrons, the effect of the threshold function must be included.

The estimate of changes to be expected in EDC on going from ferromagnetic to paramagnetic nickel depends on using the band density of states corresponding to $n(E)$ in Eq. (3) to predict changes in the optical density of states $\eta(E)$. In previous photoemission studies of noble and transition metals, it has been found that $\eta(E)$ obtained from analysis of photoemission data on the nondirect model is frequently quite similar to the calculated $n(E)$.[13,23,27] Systematic methods for determining the optical DOS from measured EDC have been described,[27] and generally this can be a somewhat complicated process. In the photon energy range of interest in the nickel experiment, $\hbar\omega = 7.7-10.7$ eV; however, it is expected that the threshold function and $\omega\sigma(\omega)$ are smoothly varying functions of E or ω. Then, in the absence of structure in the final DOS $\eta(E_i + \hbar\omega)$, the EDC reflect the occupied or valence optical DOS $\eta(E_i)$. The experimental EDC for nickel did not indicate structure in the final optical DOS.

Following this line of reasoning (the EDC reflect the optical density of states which, in turn, is similar to the band DOS), the band DOS for ferromagnetic and paramagnetic nickel can be used to obtain an idea of expected changes in experimental EDC on going from the ferromagnetic to paramagnetic state. Figure 3 plots the band DOS curves of Hodges et al.[14] after they have been convolved with a broadening function[25] to allow a better comparison with experimental results. The use of the nondirect-transition model with the DOS curves from the assumed band-calculation results in a predicted peak shift of 0.18 eV. If, instead, of employing a band calculation with a small exchange splitting, we had used one of the calculations in the literature with a larger splitting,[28–30] the calculated changes above T_C would be larger than 0.18 eV.

III. EXPERIMENT

The photoemission investigation of nickel was pioneered by Blodgett and Spicer.[31] Their EDC obtained from evaporated nickel films revealed a large peak at 4.6 eV below the Fermi level and weaker maxima at 0.3 and 2.2 eV below E_F. Subsequent experiments were carried out by Breen, Wooten, and Huen[32] and by Callcott and MacRae[33] on samples cleaned with argon bombardment and
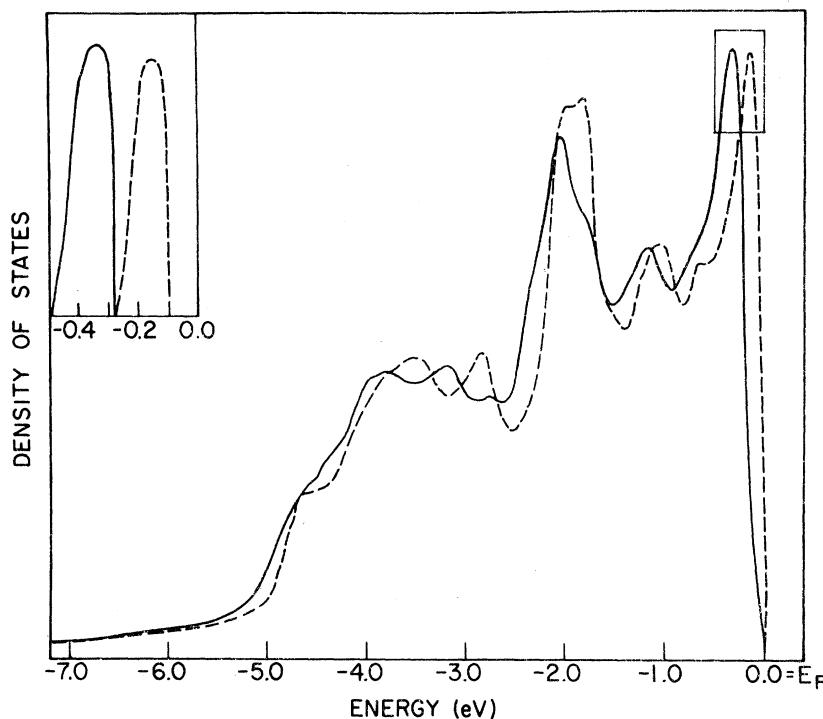
FIG. 3. Expected difference
between EDC from ferromag-
netic Ni is estimated in the non-
direct-transition model by com-
paring the density of states of
Hodges *et al.* The insert shows
a 3× magnification of the
d-band peak near E_F which, in
this model, is expected to shift
0.18 eV in going from paramag-
netic (dashed curve) to ferro-
magnetic (solid curve) Ni.

by Vehse and Arakawa[34] and Eastman[23] on evapo-
rated films. The strength of the structure varied
considerably among the different experiments.
Recently, Eastman and Cashion[35] have suggested
that the −4.6-eV peak can be explained by a peak
caused by chemisorbed oxygen which is 2 eV wide
and located at −5.5 eV. Our measured EDC from
an electron-gun-evaporated film is compared to the
measurements plotted in Fig. 4. The increased
strength of the leading peak in our curve and the
sharpness of the cutoff compared to the EDC of
Eastman is attributed primarily to our use of the
screened-emitter analyzer.[36]

During the course of our investigation, EDC were
obtained from a variety of samples, including a
heat-cleaned single crystal, a crystal cleaned by
argon bombardment and heating, an electron-beam-
evaporated film onto a Ni single-crystal substrate,
and an electron-beam-evaporated film onto a NaCl
crystal. Consistent results were obtained from all
of the samples, but it is expected that the evapo-
rated film onto the Ni substrate was the cleanest and
most perfect. Because the peak near E_F in the
EDC from a film evaporated onto Ni was somewhat
stronger than in other samples, our attention will
be focused on these results.

A $\frac{5}{8}$-in.-diam Ni single-crystal disk with the
[100] axis perpendicular to the surface was used as
a substrate for the electron-gun evaporation of the
nickel film. The substrate had been spark cut
from a single-crystal rod and then spark planed

and mechanically polished. Just before mounting
it in the photoemission flange to be put in the vac-
uum chamber, it was chemically polished follow-
ing the procedure of Tegart.[37] The substrate was
heat cleaned in ultrahigh vacuum at 500 °C for 7 h.

A Varian "e-gun" (electron-beam evaporator),
which we equipped with a specially fabricated thori-
ated-tungsten filament was used to evaporate the
99.9%-pure nickel rod. This rod was hydrogen
fired to 1200 °C before it was put in the vacuum and
then was premelted and thoroughly outgassed in
vacuum before evaporation. The chamber was
pumped with a Varian 140-liter/sec Vac Ion pump
which achieved a base pressure of 1×10^{-11} Torr.
During evaporation, the pressure rose to 1×10^{-9}
Torr for the first 2 min but was less than 5×10^{-10}
Torr during the remaining 17 min. The film thick-
ness was approximately 1500 Å as measured by a
quartz-crystal-microbalance thickness monitor
described by DiStefano.[38]

Because the preparation of consistent Ni samples
had proved so difficult (Fig. 4) in the past, we
monitored the partial pressures of the residual
gases before and during evaporation with a Varian
quadrupole residual-gas analyzer. Before evapora-
tion, we observed residual gases with mass num-
bers 2, 15, 16, 28, and 44, corresponding to H_2^+,
CH_3^+, CH_4^+, CO^+, and CO_2^+, respectively. The
same gases were present during evaporation; the
partial pressure of hydrogen relative to the other
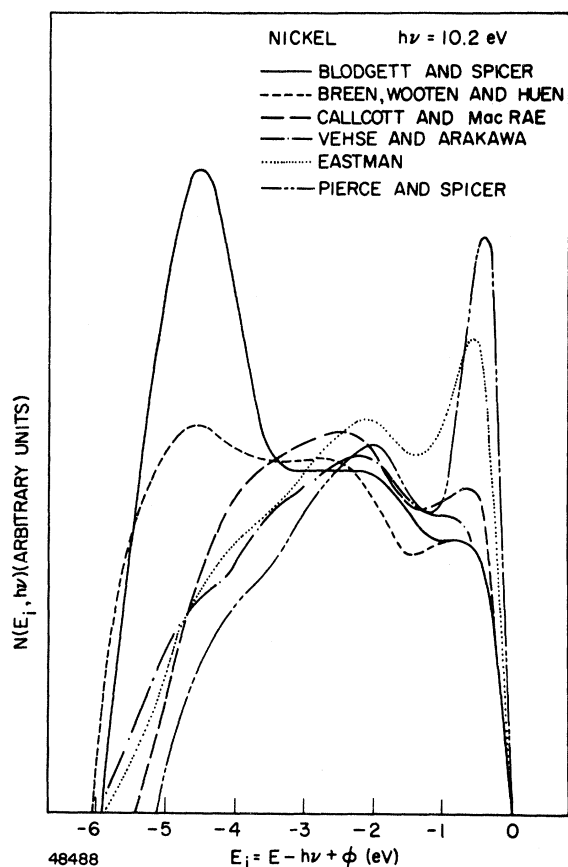constituents about doubled and the CH_3^+ and CH_4^+

FIG. 4. Encountered difficulties in obtaining clean Ni samples for photoemission experiments is illustrated by a comparison between EDC at $\hbar\omega = 10.2$ eV from the present work and the earlier work of Blodgett and Spicer; Breen, Wooten, and Huen; Callcott and MacRae; Vehse and Arakawa; and Eastman.

peaks increased slightly.

The EDC from this evaporated film are plotted in Fig. 5. The rapid rise of the leading edge to the extremely strong peak near the Fermi level is particularly striking. The position of the leading peak is 0.2 eV below E_F at $\hbar\omega = 7.7$ eV, 0.28 eV at $\hbar\omega = 10.2$ eV, and 0.4 eV at $\hbar\omega = 11.6$ eV. Over the same energy range, the leading peak rises from zero to 75% of its maximum height in 0.1, 0.17, and 0.25 eV at $\hbar\omega = 7.7$, 10.2, and 11.6 eV, respectively. The rise of the leading edge in the nickel EDC gives a measure of the over-all resolution function, and the shift in the position of the leading peak up to 10.2 eV can be understood in terms of the resolution-function shift.[24] At higher energies, the shift to lower energy may be caused in part by changes in the electronic structure. The leading peak also broadens with increasing energy; its full width halfway between its top and the valley is 0.3 eV at $\hbar\omega = 7.7$ eV, 0.5 eV at $\hbar\omega = 10.2$ eV, and 0.55 eV at $\hbar\omega = 11.6$ eV. The above estimates

of the resolution function at these energies indicate that approximately one-half of the broadening is due to instrumental effects and the other half to changes in the excited-electron distribution in the metal.

A broad maximum obscured by the threshold function at lower photon energies occurs at approximately 2.1 eV below E_F. The absence of a low-energy peak even at photon energies greater than 11 eV indicates that surface contamination was minimal. In the figures, the straight portion of the leading and trailing edges of the EDC is extrapolated
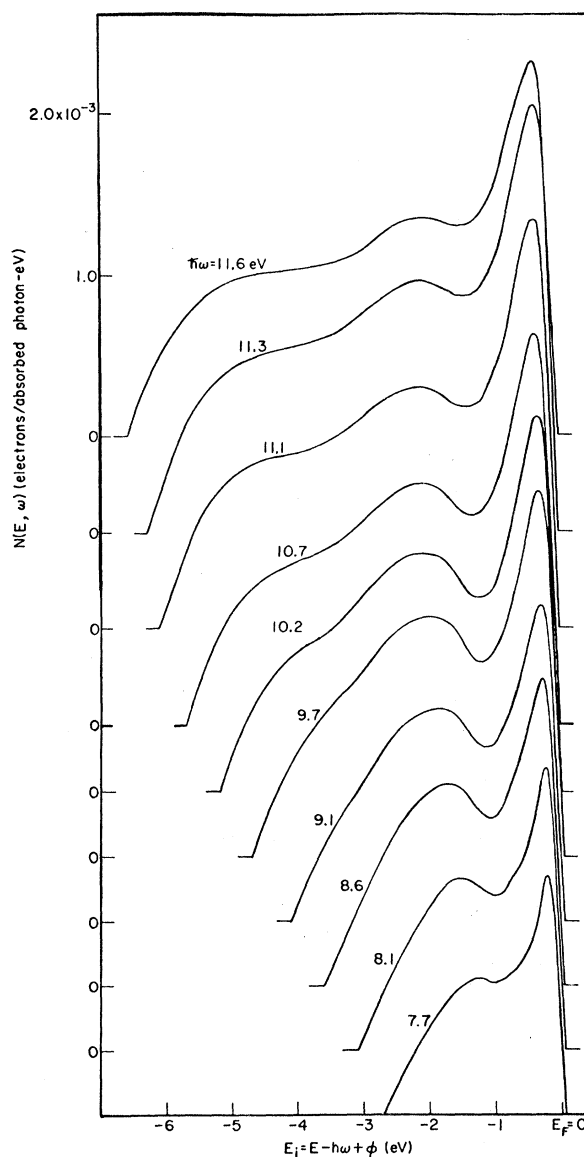

FIG. 5. EDC from a Ni film electron-gun evaporated in ultrahigh vacuum onto a single-crystal Ni substrate. The screened-emitter analyzer has resolved the variation in peak width and the sharp cutoff at the Fermi level.

T$_I$: UTC 0-6
PRIMARY 15 k
SECONDARY 45 k CT
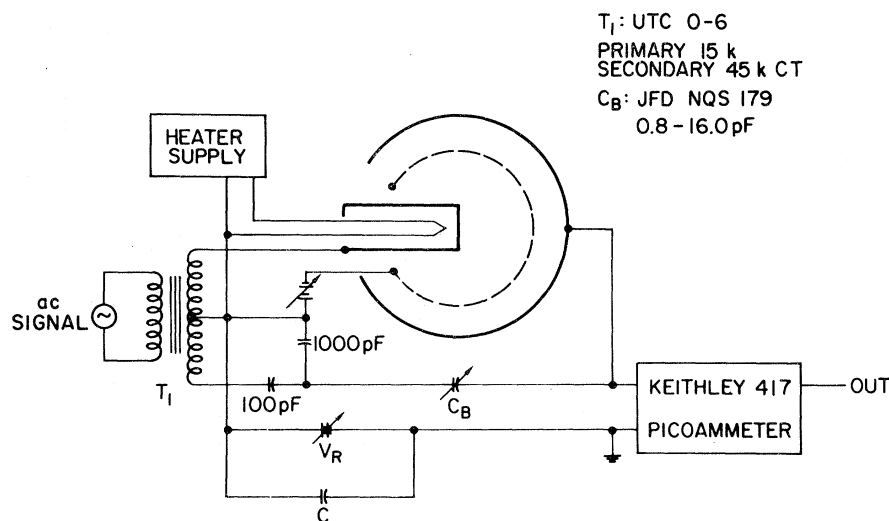C$_B$: JFD NQS 179
    0.8 - 16.0 pF

FIG. 6. Circuit used with the screened-emitter analyzer to obtain the EDC at 678 °K. The collector current is measured and the heater is grounded with respect to ac disturbances through the capacitor C.

with a straight line to the baseline. The experimental curves have a slight instrumental rounding at the baseline, as seen in the actual recorder traces.[36]

The magnetization of nickel is maximum at 0 °K and decreases to zero at the Curie temperature $T_C = 631$ °K. Magnetization at room temperature is 95% of the maximum value. On the basis of the band model in which the band splitting is proportional to magnetization, significant changes in the EDC would be expected even in going from room temperature to just below T_C, where the magnetization is small. The change from room temperature rather than slight differences from T_C is significant; nevertheless, in our high-temperature experiment, we aimed for 50 °C above T_C.

To the best of our knowledge, these were the first successful EDC measurements at such high temperatures. The major difficulty is to maintain the sample at high temperature while making photoemission measurements. Continuous heating with an ac heater is not acceptable because the electronic noise it introduces disrupts the measurements of small ($\approx 10^{-11}$ A) photoemission currents. Heating the sample with a regulated dc current in a noninductive heater proved successful. Normal ac ripple and pickup would be intolerable if the energy analyzer is used in the conventional way to measure emitter current. However, with the screened-emitter analyzer, it is most natural to measure collector current, as shown in the circuit diagram in Fig. 6. Noise from the heater supply is passed through the large capacitor C. Although the noise at the picoammeter output is a few times larger than for room-temperature measurements, the picoammeter can be kept on a sensitive scale without overloading. The remaining ac ripple is further rejected by using an even subharmonic of

60 Hz as the reference frequency for the PAR lock-in amplifier.[38] The key factor in obtaining good high-temperature measurements with the dc heater is that it was essentially connected to ground with regard to ac disturbances.

The temperature was monitored with a chromel-alumel thermocouple mounted in the copper sample holder $\frac{1}{32}$ in. behind the Cu-Ni interface. In a separate calibration experiment, the temperature at the front of a polished nickel substrate was measured by a chromel-alumel thermocouple, brazed to it and compared to measurements from the thermocouple just behind the Cu-Ni interface. It was found that a temperature of 678 °K at the sample surface corresponded to a temperature of 688 °K in the sample holder. The temperature at the sample surface followed that of the sample holder closely, that is, an equilibrium between the two was quickly attained. The collector temperature changed slowly because of radiation from the emitter assembly; for example, the collector temperature increased from room temperature to 60 °C in $2\frac{1}{2}$ h when the sample was at 678 °K.

Figure 7 plots EDC from the evaporated film at 678 °K (dashed curve) and after it had cooled to room temperature 295 °K (solid curves). The room-temperature EDC before heating (Fig. 5) differ from those after heating only in that the leading peak is 10% to 15% stronger. The pressure remained less than 5×10^{-11} Torr during the high-temperature measurements.

When examining the experimental EDC and comparing them to calculations, we shall pay particular attention to the peak near the high-energy cutoff; this peak results from transitions originating in bands near the Fermi level. We focus on this peak because (i) this is the sharpest available experimental structure; (ii) it can be followed over
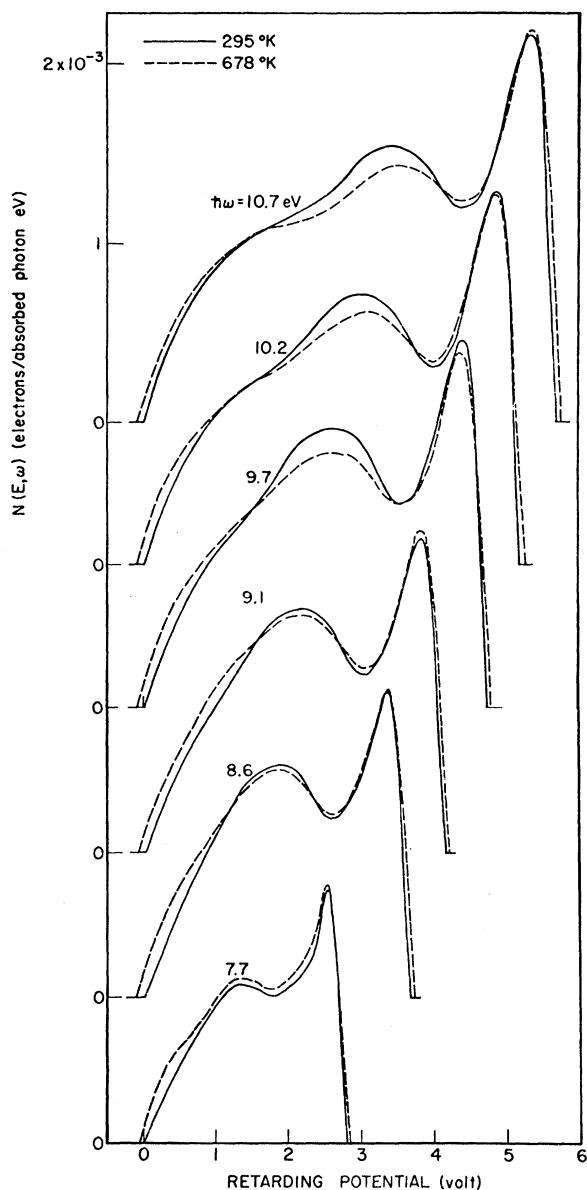
FIG. 7. EDC from the evaporated film in Fig. 5 while at 678 °K (dashed curves) and after cooling to room temperature 295 °K (solid curves). The leading peak originating from d states near the E_F does not shift in going from paramagnetic to ferromagnetic Ni within our experimental uncertainty of ± 0.05 eV.

the widest range of photon energy (more than 3 eV); (iii) it is strong in all of the calculated EDC; and (iv) it corresponds to a well-defined peak in the DOS (Fig. 3).

As can be seen from Fig. 7, there is no change in the position of the leading peak in going from ferromagnetic to paramagnetic nickel. An upper limit on any such change is placed at the experimental uncertainty of ±0.05 eV. The location of the second peak is somewhat less certain (~ ±0.15

eV) because it is broader and because of slight distortions resulting from a small low-energy-background current which had to be subtracted from the high-temperature curves. Thermal broadening of the Fermi surface is directly observed in the 0.05–0.1 eV increase in the leading-edge cutoff of the high-temperature EDC.

Extreme care was taken in comparing EDC at 295 and 678 °K in our search for the peak shifts predicted by the band model of ferromagnetism; for example, any error in monochromator resolution was the same at both temperatures. Typically the half-width at half-maximum of the power spectrum from the monochromator was 0.05–0.075 eV; where possible, this was improved by tuning in on a peak of the hydrogen discharge spectrum. Similar care was taken to ensure that errors caused by electronic instrumentation, in particular the magnitude of the ac voltage which was typically 0.1– 0.15 V peak-to-peak, were the same in the curves to be compared. We have assumed implicitly that resolution errors of the energy analyzer were the same at corresponding photon energies for both room- and high-temperature EDC. The magnetic field in the collector region resulting from the magnetism of the sample was found to be much less than $\frac{1}{10}$ of the earth's field.

In comparing peak positions in EDC at different temperatures, a potential source of error is a change in the collector work function; however, the vacuum was very good throughout the high-temperature measurements and the collector heated less than 100 °C which gave us no reason to suspect a change in the collector work function. In addition, the collector work function can be monitored, because the difference between the point of intercept of the trailing edge of an EDC with the baseline and the point on the baseline corresponding to zero-applied retarding voltage is the work-function difference between the collector and sample. The difference in the work function (discussed below) of the nickel film at 295 and 678 °K is 0.1±0.06 eV which corresponds to the change of 0.1 eV in the trailing-edge intercept and suggests that the collector work function did not change. This analysis suggests that the maximum upper limit on a change of the collector work function is ±0.06 eV plus the difficult to estimate uncertainty (a few hundreths of an eV) in locating the trailing-edge intercept. There is little cause for a change in collector work function in a single data set; it was checked by repeating curves and by taking curves that were to be compared close together in time. The difference in emitter-collector contact potential due to thermal emf is less than 0.01 eV. All factors taken together led us to place an upper limit of ±0.05 eV on the uncertainty in measuring a shift in the position of the leading peak in com-
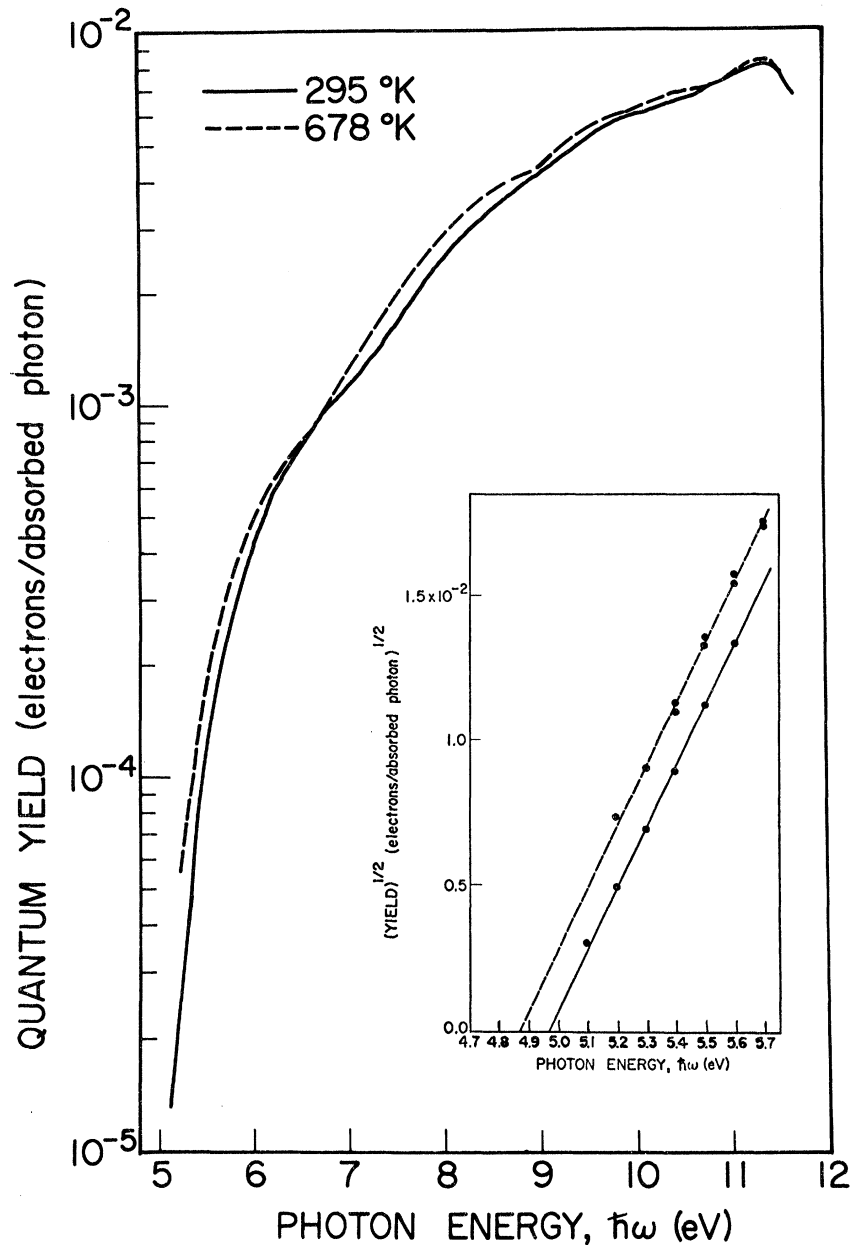
FIG. 8. Quantum yield of paramagnetic (dashed curve) and ferromagnetic (solid curve) Ni. The insert shows the Fowler-plot determination of the work functions.

paring high-temperature and room-temperature EDC. The sharpness of the leading peak presented no difficulty in locating its position, but the broader peak at -2.0 eV below E_F could only be located with an uncertainty of ± 0.15 eV.

The quantum yield at 295 and 678 °K was used to normalize the EDC, and a Fowler plot[39] of this yield determined the work functions. The photocurrent to the positively biased collector was compared to the photocurrent from a calibrated Cs_3Sb photodiode that could be inserted in the incident monochromator beam to measure its intensity. When corrections for the transmission of the vacu-

um-chamber window T_w and the reflectivity of the sample R are included, the absolute quantum yield is obtained in electrons per absorbed photon,

$$Y = I(\text{sample}) \, Y(\text{standard})/I(\text{standard}) \, T_w(1 - R).$$

Figure 8 shows the yield from this evaporated Ni film at room temperature (solid curve) and at high temperature (dashed curve). The work functions determined from a Fowler plot of the quantum yield are 4.87 ± 0.04 eV at 678 °K and 4.97 ± 0.02 eV at 295 °K (Fig. 8). The measurement of the small photocurrent near threshold was more difficult at high temperatures because of the greater elec-

tronic noise. The same values of the work function were obtained when the full temperature-dependent Fowler theory[39] was used.

Previous measurements obtained by Cardwell[40] and Ames and Christensen[41] from nickel for $\hbar\omega$ = 5.0–5.5 eV also showed an increase in yield with temperature in this range. At $\hbar\omega$ = 5.2 eV, for example, Cardwell found the yield to double in going from 300 to 623 °K. In both of these investigations, measurements were made on nickel ribbons that had been heat cleaned for over two months. Ames and Christensen flashed the ribbon to 1200 °C before each set of yield measurements. In contrast to our results, these investigators found a slight increase of work function with temperature as determined from temperature-dependnet Fowler plots. Cardwell measured work functions of 5.06, 5.05, and 5.1 eV at temperatures 300, 623, and 770 °K, respectively; Ames and Christensen measured work functions of 5.08, 5.07, 5.08, 5.09, 5.10, 5.09, and 5.13 eV with an accuracy of ± 0.03 eV at temperatures of 298, 443, 523, 563, 613, 633, and 833 °K, respectively.

IV. DISCUSSION

The striking result of our experiment is that none of the changes in the experimental high-temperature EDC predicted above in terms of the band model of magnetism were detected within our experimental uncertainty of ±0.05 eV. The leading peak in the paramagnetic EDC, calculated assuming direct transitions, was predicted to shift 0.25 eV relative to the leading peak of the ferromagnetic EDC over the range $\hbar\omega$ = 7.7 eV to 10.7 eV; a 0.18-eV shift of this peak was also predicted by the nondirect-transition model. The magnitude of the peak shifts are such that they would be easily observable in our experiment. On the basis of arguments to be given below, we would like to suggest that the Slater-Stoner-Wohlfarth band theory is not sufficient to describe the observed photoemission from ferromagnetic and paramagnetic nickel.

The results of our experiment are in agreement with the recent measurements by Rowe and Tracy,[8] which determine with very high resolution the d-band-peak position in EDC from cesiated Ni at low photon energies. These measurements are complementary to ours for clean Ni at higher photon energies. Although we do not locate the d-band position as accurately as Rowe and Tracy, the shape and amplitude of the EDC from Ni above T_C can be seen from our measurements. Using a servo method they developed to accurately monitor the d-band peak relative to E_F as a function of temperature, Rowe and Tracy found a peak shift between room temperature T_C of approximately 45 MeV and between room temperature and 670 °K of 35–40 MeV. Over the same temperature range,

the Pd d-band EDC peak was found to shift approximately 50 MeV in the opposite direction presumably because of the effects of electron-phonon interaction and volume expansion. If effects of similar magnitude are present in Ni, the magnetic shift of the Ni EDC peak is really 0.09 eV.[8] In other words, electron-phonon interaction and volume-expansion effects would reduce the magnitude of the peak shifts, that one would expect to measure from our minimum value of 0.18 eV, calculated for nondirect transitions to 0.13 eV. A similar reduction is also expected in the 0.25-eV shift calculated for direct transitions. Thus, the minimum expected peak shift that we calculated (0.13 eV including these thermal effects) is still three times larger than the 0.04-eV peak shift measured by Rowe and Tracy. The band model does not explain the experimental observations. In addition, the temperature dependence of the d-band peak near T_C reveals a cusp[8] similar to the specific-heat anomaly; this critical behavior is suggestive of many-body effects outside of the band picture.

At the time when our experimental results were first reported, the band model of magnetism received a further challenge from the measurements of Bänninger et al.[9] who found a + 15% spin polarization for photoelectrons emitted from near the Ni Fermi level. In contrast, most band structures of Ni predict a negative polarization [magnetic moment of the photoelectrons antiparallel to the direction of magnetization corresponding to a predominance of minority (down) spins] at E_F. Wohlfarth[42] has shown that the negative-polarization region in Ni may be so narrow as to be undetected by the experiment. An alternative explanation for the positive polarization has been suggested by Smith and Traum[43] who calculated the expected spin polarization by assuming direct transitions and the band structure of Hodges et al. Subsequent measurements on Co[44] provided a more stringent test for the band model of magnetism and suggested that it does not adequately explain the spin-polarized photoemission results.

We note that not only the absence of the expected d-band peak shifts but also the similarity in shape and magnitude of the d-band peak above and below T_C places significant constraints on interpretations based on the band model. Wohlfarth's explanation of spin-polarized photoemission results was based on a model in which the majority-spin d-band edge to E_F energy difference is 0.060 eV and the leading peak of the minority-spin band is above E_F.[42] His schematic model, however, predicts a leading peak in the paramagnetic density of states that is 25% higher than in the ferromagnetic case; no manifestation of such a change in the DOS is seen in the EDC.

Since the first report of our results, Anderson,[45]

Baltensperger,[46] and Doniach[47] have calculated that many-body effects may be of the right magnitude to explain the small temperature dependence of the d-band peak and also the positive spin polarization for Ni observed by Bänninger et al.[9] Anderson states that the renormalization required by strong interparticle correlations makes the simple Hartree-Fock ground state no longer appropriate. Baltensperger found that it may be energetically favorable for the electrons to form a coherent state such that it costs more energy to excite a minority electron than a majority electron. This calculation qualitatively explains the small temperature dependence of the d-band peak and the observed positive spin polarization and further suggests that the width of the d bands in a photoemission experiment should be less than the width from a band calculation. The Hartree-Fock ground state is not changed in Doniach's calculation[47] which focuses on the excitation process. More energy is required to excite a minority- than a majority-spin electron, because the electrons in the full majority-spin band cannot relax around a hole in the minority-spin band; in contrast, minority-spin electrons can relax around a hole in the majority. The "relaxed orbital correction" caused by electrons relaxing around the hole left by a photoexcited electron is therefore different for majority and minority spins and is of such a magnitude as to counterbalance the exchange splitting. In this case, because photoemission and optical measurements do not sense the magnetic ground state, the peak shifts calculated in Sec. II would not be observed. Harrison[48] has suggested that local moments also exist above the Curie temperature. In this qualitative picture, increasing the temperature above T_C causes disordering of the local moments formed from resonant states[49] on each atom, and changes in the EDC would only be expected to be on the order of $k_B T_C$ unless ferromagnetism is important to the stability of the formation of the moments.

It should be noted that when many-body explanations are used in connection with the ferromagnetism of Ni, the description of optical excitations in terms of one-electron k-conserving transitions becomes questionable and the nondirect model may represent a better approximation. A discussion of this was presented by Spicer.[13]

Before describing the apparent conflict between our conclusions and the results of optical absorption and neutron-scattering experiments, we anticipate and answer two minor objections to our interpretation that might be raised. The first is whether the band structure of Hodges et al.[14] is sufficiently accurate to predict the EDC peak shifts. From photoemission measurements at $\hbar\omega = 40$ eV, Eastman[21] has estimated the Ni bandwidth to be 3.3 eV in approximate agreement widths of 3.0[50] and 2.7

eV,[51] as determined from the lower resolution x-ray photoelectron spectroscopy measurements, but narrower than the 4 to 5-eV widths estimated from our EDC at lower energy.

In attempting to obtain bandwidths from EDC, one should be aware of an unresolved problem. This is the possibility that the electronic structure changes as one approaches the surface. This is important because the depth of escape of the unscattered electrons decreases as the photon energy increases.[12,22,23,27] For Ni, the escape depth is approximately 10 Å at 8 eV; thus, it may become very small at 40 eV or in the x-ray region. The band narrowing noted above, therefore, may not reflect bulk electronic structure but, instead, may be the result of a narrowing of the bands at the surface. Further experimental work should resolve this problem.

If the 3.3-eV width is taken to be correct instead of the 4.8-eV width of the band structure of Hodges et al.,[14] the predicted peak shifts could be approximately 30% smaller but still experimentally detectable. The d-band splitting in the Hodges band structure (0.29-eV average, 0.37 eV at E_F) is smaller than the 0.4 to 0.6-eV splitting in the calculation of Zornberg,[30] the 0.8-eV average splitting of Connolly,[29] and the 0.7-eV splitting of Wakoh and Yamashita.[28] Because other band structures have up to double the exchange splitting of the band structure we used, the peak shifts predicted from our calculations tend to be conservative.

The second possible objection is that, at room temperature, two atomic layers at each interface of the Ni film may be magnetically dead, as reported by Liebermann et al.[52] The magnetically dead layers observed in films formed by electroplating from aqueous solution[52] may not be present in our samples which were films electron-gun evaporated in ultrahigh vacuum and a single crystal cleaned by heating and argon bombardment. If one assumes two magnetically dead layers corresponding to 3.5 Å on the (100) surface of Ni and, as above, an electron-electron–scattering length of 10 Å for electrons with energy at 8 eV above E_F, then $1 - e^{-3.5/10}$ or 30% come from the "dead" layers. These "paramagnetic" electrons in the ferromagnetic film would tend to reduce the predicted peak splitting, but it would still be observable. Whether such dead layers really exist in our samples is an open question. In measurements of the spin polarization of photoelectrons from electron-gun evaporated Ni films as a function of magnetic field strength, Bänninger et al.[9] found no evidence of paramagnetic electrons. That the dead layers exist in electrolytically deposited films has been disputed by the recent Mössbauer measurements of Shinjo et al.[53]

Shiga and Pells[10] have interpreted the measurements of the temperature dependence of the optical absorption spectrum of Ni in terms of a temperature-dependent exchange splitting of the energy bands. The primary experimental peak at $\hbar\omega = 4.8$ eV narrows approximately 0.13 eV as the temperature is increased from 295 to 670 °K. Shiga and Pells suggest that the shape of this peak can be explained by a superposition of two peaks separated by an energy that is proportional to the spontaneous magnetization. The key point in this explanation is their assignment of the peak at 4.8 eV to transitions from the spin-split bands at L_2' to the unsplit or negligibly split conduction bands at L_{12}. If this explanation is correct, it is surprising that no significant change was seen in the leading EDC peak that originates from states at the top of the d bands. In fact, the analogous optical absorption peak in Cu is a composite of transitions from the low-lying d bands at L and X to states just above E_F and of transitions from L_2' to L_{12}.[26] Gerhardt[54] has suggested that approximately 30% of the Cu peak is the result of L_2' to L_{12} transitions and Seib and Spicer[55] have argued that only 10% is caused by L_2' to L_{12} transitions. Assuming direct transitions in the band structure of Hodges et al., our calculation of $D(E, \omega)$ for Ni show that over 70% of the transition strength at $\hbar\omega = 4.8$ eV is due to transitions from low-lying d-bands to minority-spin bands just above E_F. For such transitions, the band model predicts a very small temperature-dependent effect in the optical absorption, because the change in splitting of the low-lying bands and the band at E_F is similar. Unfortunately, with photon energies to 11.6 eV, transitions from the low-lying bands are still obscured in photoemission by the escape function. The relaxed orbital corrections suggested by Doniach[47] appear to explain the photoemission data and would be expected to reduce the manifestations of the spin-split bands in the optical absorption data. In our opinion, the optical data cannot be explained adequately by a straightforward application of the band model.

Komura et al.[11] have measured the spin-correlation function in Ni by means of neutron scattering over a temperature range of 0.5–1.6 T_C. Spin-wave excitations are distinctly evident at room temperature and become less pronounced at higher temperatures. In contrast to our results, which have not been adequately explained by the band model, the neutron data are well explained by the calculations of the response function $X(\vec{k}, \omega)$ in which the band splitting is assumed to change with temperature and disappear above T_C.[56,57] However, between the experimental scattering data and the change in the exchange splitting of the bands, lie extensive calculations which, in fact, were reported to be not critically dependent on the band structure. The different conclusions reached concerning the band model can be understood when the varying nature of the two experiments is considered. The many-body effects suggested by Anderson[45] and Doniach[47] can be applied to the photoemission experiment where an electron is excited 7 eV or more to a conduction-band state in approximately 10^{-15} sec. The situation in the neutron-scattering experiment is much different; the energy change is nearer 0.1 eV in the spin-flip process and the interaction period is approximately 100 times longer.

In conclusion, the band model of ferromagnetism that predicts a d-band peak shift of ≈ 0.2 eV is not consistent with our experimental results which show that any shift must be smaller than ± 0.05 eV. Because the band model does not explain the spin-polarized photoelectron results[9] (the photoemission results of Rowe and Tracy[8] or our results), we must seek extensions of this model or new models. It appears that the suggested many-body effects may be crucial to our understanding of magnetism in Ni.

ACKNOWLEDGMENTS

*Work supported by the U. S. Army Research Office, Durham, and by the Advanced Research Projects Agency through the Center for Materials Research, Stanford University.

†Present address: Laboratory of Solid State Physics, Swiss Federal Institute of Technology, CH-8049 Zurich, Switzerland.

[1]D. T. Pierce and W. E. Spicer, Phys. Rev. Letters 25, 581 (1970).

[2]J. C. Slater, Phys. Rev. 49, 537 (1936); 49, 931 (1936).

[3]E. C. Stoner, Proc. Roy. Soc. (London) A154, 656 (1936); A165, 372 (1938).

[4]E. P. Wohlfarth, Rev. Mod. Phys. 25, 211 (1953).

[5]E. P. Wohlfarth, in Proceedings of the Nottingham Conference on Magnetism, 1964 (The Institute of Physics and the Physical Society, London, 1965), p. 51.

[6]J. C. Phillips, J. Appl. Phys. 39, 755 (1968).

[7]C. Herring, in Magnetism, edited by G. T. Rado and H. Suhl (Academic, New York, 1966), Vol. IV.

[8]J. E. Rowe and J. C. Tracy, Phys. Rev. Letters 27, 799 (1971).

[9]U. Bänninger, G. Busch, M. Campagna, and H. C. Siegmann, Phys. Rev. Letters 25, 585 (1970).

[10]M. Shiga and G. P. Pells, J. Phys. C 2, 1847 (1969).

[11]S. Komura, R. D. Lowde, and C. G. Windsor,

Neutron Elastic Scattering (International Atomic Energy Agency, Vienna, Austria, 1968), Vol. 2, p. 101.

[12]C. N. Berlgund and W. E. Spicer, Phys. Rev. 136, A1030 (1964).

[13]W. E. Spicer, Phys. Rev. 154, 385 (1967).

[14]L. Hodges, H. Ehrenreich, and N. D. Lang, Phys. Rev. 152, 505 (1966); and L. Hodges, Ph.D. thesis (Harvard University, 1966) (unpublished).

[15]H. Ehrenreich and L. Hodges, *Methods in Computational Physics*, edited by B. Adler, S. Fernbach, and M. Rotenberg (Academic, New York, 1968), Vol. 8, p. 149.

[16]J. Hanus, MIT Solid State and Molecular Theory Group, Quarterly Progress Report No. 44, 1962 (unpublished).

[17]N. V. Smith, Phys. Rev. Letters 23, 1452 (1969).

[18]N. V. Smith, Phys. Rev. B 3, 1862 (1971).

[19]J. F. Janak, D. E. Eastman, and A. R. Williams, Solid State Commun. 8, 271 (1970).

[20]A. R. Williams, J. F. Janak, and V. L. Moruzzi (unpublished).

[21]D. E. Eastman, *Proceedings of the International Conference on Electron Spectroscopy, California, 1971* (North-Holland, Amsterdam, 1972), Chap. IV, p. 487.

[22]E. O. Kane, Phys. Rev. 159, 624 (1967).

[23]D. E. Eastman, J. Appl. Phys. 40, 1387 (1969).

[24]T. H. DiStefano and D. T. Pierce, Rev. Sci. Instr. 41, 180 (1970).

[25]As shown in Ref. 24, an appropriate broadening function causes the structure to be both broadened and lowered in energy. The broadening functions used in Figs. 1 and 2 causes a δ function to be shifted -0.15 eV and broadened to 0.32-eV full width at half-maximum (FWHM). The broadening function in Fig. 3 shifts a δ function -0.1 eV and broadens it to 0.16-eV FWHM.

[26]F. M. Mueller and J. C. Phillips, Phys. Rev. 157, 600 (1967).

[27]W. F. Krolikowski and W. E. Spicer, Phys. Rev. 185, 882 (1969).

[28]S. Wakoh and J. Yamashita, J. Phys. Soc. Japan 19, 1342 (1964).

[29]J. W. D. Connolly, Phys. Rev. 159, 415 (1967).

[30]E. I. Zornberg, Phys. Rev. B 1, 244 (1970).

[31]A. J. Blodgett and W. E. Spicer, Phys. Rev. 146, 390 (1966); A. J. Blodgett, Ph.D. thesis (Stanford University, 1965) (unpublished).

[32]W. M. Breen, F. Wooten, and T. Huen, Phys. Rev.

152, 505 (1967).

[33]T. A. Callcott and A. U. MacRae, Phys. Rev. 178, 966 (1969).

[34]R. C. Vehse and E. T. Arakawa, Phys. Rev. 180, 695 (1969).

[35]D. E. Eastman and J. K. Cashion, Phys. Rev. Letters 27, 1520 (1971).

[36]D. T. Pierce and T. H. DiStefano, Rev. Sci. Instr. 41, 1740 (1970).

[37]W. J. Tegart, *The Electrolytic and Chemical Polishing of Metals* (Pergamon, London, 1960), p. 102.

[38]T. H. DiStefano, Ph.D. thesis (Stanford University, 1970) (unpublished).

[39]R. H. Fowler, Phys. Rev. 38, 45 (1931).

[40]A. B. Cardwell, Phys. Rev. 76, 125 (1949).

[41]J. Ames and R. L. Christensen, IBM Res. Develop. 7, 34 (1963).

[42]E. P. Wohlfarth, Phys. Letters 36A, 131 (1971).

[43]N. V. Smith and M. M. Traum, Phys. Rev. Letters 27, 1388 (1971).

[44]G. Busch, M. Campagna, and H. C. Siegmann, Phys. Rev. B 4, 746 (1971).

[45]P. W. Anderson, Phil. Mag. 24, 203 (1971).

[46]W. Baltensperger, Summer School at McGill University, Montreal, Canada, 1971 (unpublished).

[47]S. Doniach, International Conference on Magnetism, Chicago, 1971 (unpublished).

[48]W. A. Harrison, *Solid State Theory* (McGraw-Hill, New York, 1970), p. 485.

[49]P. W. Anderson, Phys. Rev. 124, 41 (1961).

[50]C. S. Fadley and D. A. Shirley, Proceedings of the Electronic Density of States Symposium, National Bureau of Standards, Washington, D. C., 1969 (unpublished).

[51]Y. Baer, P. F. Heden, J. Hedman, M. Kalasson, C. Nordling, and K. Siegbahn, Physica Scripta 1, 55 (1970).

[52]L. Liebermann, J. Clinton, D. M. Edwards, and J. Mathon, Phys. Rev. Letters 25, 232 (1970).

[53]T. Shinjo, T. Matsuzawa, T. Takada, S. Nasu, and Y. Murakami, Phys. Letters 36A, 489 (1971).

[54]U. Gerhardt, Phys. Rev. 172, 651 (1968).

[55]D. H. Seib and W. E. Spicer, Phys. Rev. 187, 1176 (1969).

[56]C. G. Windsor, R. K. Lowde, and G. Allan, Phys. Rev. Letters 22, 849 (1969).

[57]R. D. Lowde and C. G. Windsor, Advan. Phys. 19, 813 (1970).